Plasma Membrane TRPV4 Relocalization as a Mechanosensitive Prognostic Biomarker in Ductal Carcinoma In Situ

Christopher Chan[1], Elham Arbzadeh[2], Shabnam Samankan[2], Patricia Latham[2], Arnold Schwartz[2], Rachel Du[1,3], Inhee Chung[1,4,*]

Affiliations:

1 Department of Anatomy and Cell Biology, School of Medicine and Health Sciences, George Washington University, Washington, DC, USA
2 Department of Pathology, George Washington Medical Faculty Associates, Washington, DC, USA
3 Thomas Jefferson High School for Science and Technology, Alexandria, VA, USA
4 Department of Biomedical Engineering, GW School of Engineering and Applied Science, George Washington University, Washington, DC, USA

[*] Corresponding author

Abstract

Purpose: Reliable prediction of invasive progression remains an unmet need in ductal carcinoma in situ (DCIS). Conventional histologic grading provides limited prognostic value. Building on mechanistic evidence that cell crowding in confined ducts engages a TRPV4-dependent mechanotransduction program, we evaluated plasma-membrane TRPV4 (PM-TRPV4) localization as a mechanosensitive, patient-level prognostic biomarker for progression to invasive ductal carcinoma (IDC).

Experimental Design: In a retrospective single-institution case-control study, we analyzed 44 patients with pure DCIS (24 progressed to IDC, 20 remained disease-free ≥5 years). Three board-certified pathologists independently scored PM-TRPV4 on whole-slide immunohistochemistry using a prespecified five-level membrane-localization rubric (linear-weighted Fleiss' κ=0.823, 95% CI 0.777–0.863). The primary endpoint was IDC-free survival assessed by Kaplan–Meier and Cox models with prespecified adjustment for histologic grade and ER status.

Results: PM-TRPV4 positivity was associated with inferior IDC-free survival (log-rank p=0.040). In multivariable Cox models, PM-TRPV4 remained independently prognostic (adjusted HR=3.77; 95% CI 1.01–14.12; p=0.049) after accounting for grade and ER, whereas histologic grade itself was not prognostic (p=0.57). Exploratory analyses in lower-grade DCIS showed larger effect sizes (OR=10.50, p=0.016; HR=3.24, p=0.086), identifying a high-risk subset with 77.8% progression versus 25.0% in PM-TRPV4-negative cases.

Conclusions: PM-TRPV4 provides independent, mechanism-informed prognostic information beyond histologic grade and ER. Given the small, single-center case-control design, findings are hypothesis-generating and support multi-institutional validation with standardized staining/scoring, external calibration, and ≥10-year surveillance, particularly to refine risk in lower-grade DCIS, where clinical decisions are most uncertain.

Translational Relevance Statement: Current DCIS management relies on histologic grade, which has variable reproducibility and offers little guidance for about 60% of patients with lower-

grade disease. We show that plasma-membrane relocalization of TRPV4 (PM-TRPV4), a functional readout of pro-invasive mechanotransduction in crowded ducts, adds independent prognostic information beyond grade and ER. In our cohort (N=44; 24 events), PM-TRPV4 positivity was associated with shorter IDC-free survival and remained significant in multivariable models (adjusted HR ~3.8; p ~0.05), whereas grade was not prognostic. Exploratory analyses suggested larger effects in lower-grade DCIS (OR ~10.5), identifying a subset at high risk (77.8% vs 25.0% progression). PM-TRPV4 achieved near-perfect inter-rater reliability (weighted kappa = 0.82) using standard IHC on routine FFPE sections, supporting practical deployment. If externally validated with standardized protocols and at least 10 years of surveillance, PM-TRPV4 testing could enable personalized risk stratification and help select lower-grade DCIS patients for active surveillance versus those requiring escalation.

Introduction

Ductal carcinoma in situ (DCIS) is a non-invasive breast neoplasm that challenges clinical decision-making because risk of progression to invasive ductal carcinoma (IDC) remains difficult to predict for the >60,000 women diagnosed annually in the United States (1-4). This uncertainty contributes to overtreatment of indolent lesions and insufficient escalation for high-risk disease. Histologic grading, based on nuclear morphology, architecture, and necrosis, provides some prognostic information but shows only moderate interobserver reproducibility (κ ~0.4–0.6) and limited accuracy for predicting progression (5-14). The problem is most acute in lower-grade DCIS (intermediate + low), which represents ~60% of cases (12,15,16), where morphology alone offers limited guidance, because some lesions still invade (17,18). Biomarkers that discriminate risk within this large subgroup could enable more personalized management.

Emerging evidence points beyond morphology to microenvironmental and patient-level biology. Extracellular matrix remodeling has been linked to progression (19,20); molecular programs associate with outcomes (21); and biomarker profiles predict invasive events after DCIS diagnosis (17,18). Active-surveillance trials (COMET, LORD, LORIS) demonstrate feasibility in carefully selected low-risk DCIS, underscoring the need for robust biomarkers to support de-escalation where appropriate (22-25). Genomic tools such as DCISionRT can inform radiotherapy decisions (26) but require specialized assays and may be less accessible, motivating complementary biomarkers measurable on routine FFPE sections.

Guided by recent work from our group, we hypothesize that mechanical stress responses provide a biological basis for DCIS progression risk (27). In confined ductal spaces, epithelial cell crowding inactivates the mechanosensitive calcium-permeable channel TRPV4 (28,29) at the plasma membrane (PM), lowering intracellular calcium, altering cell mechanics (shrinkage and stiffening), and promoting invasive behaviors (27,30). Critically, this disrupted ion homeostasis drives compensatory relocalization of inactive TRPV4 from intracellular compartments to the PM, where it is poised for reactivation under future mechanical cues (27). This mechanosensing-driven PM relocalization, distinct from constitutive membrane localization or total TRPV4 expression, provides a functional readout of pro-invasive mechanotransduction pathway engagement. We therefore evaluate PM-TRPV4 relocalization as a dynamic, mechanism-based biomarker that may complement morphology-based grading for risk stratification in DCIS. By capturing stress-induced cellular responses rather than static features, PM-TRPV4 may improve prognostic discrimination, particularly in lower-grade disease (12,15,16), helping reduce unnecessary treatment in low-risk patients while ensuring appropriate intervention for high-risk cases.

In this case-control retrospective study, our objectives were to (i) assess the association between PM-TRPV4 status and time to IDC progression; (ii) determine whether PM-TRPV4 provides prognostic information independent of histologic grade and estrogen receptor (ER) status; and (iii) evaluate performance across grade strata, with emphasis on lower-grade DCIS, where clinical utility is most needed. Because PM-TRPV4 was hypothesized to reflect a patient-level mechanosensing state, invasive events were analyzed irrespective of laterality (ipsilateral or contralateral), and prespecified sensitivity analyses evaluated potential confounding by treatment selection and event side.

Materials and Methods

Study design and ethical oversight

We conducted a retrospective case-control study at George Washington University comparing patients with pure ductal carcinoma in situ (DCIS) who subsequently developed invasive ductal carcinoma (IDC) cases with patients who remained disease-free (controls). Group assignment (case vs control status) was determined by clinical outcome rather than randomization, as appropriate for a retrospective case-control design. Sample size was determined by availability of eligible cases with adequate tissue quality and documented outcomes from the biorepository. No formal a priori power calculation was performed, as this was an exploratory biomarker discovery study designed to generate hypotheses for validation in larger cohorts. The study was approved by the George Washington University Institutional Review Board (protocol NCR203065) with a waiver of informed consent for archived tissue and de-identified clinical data.

Patient cohort and tissue procurement

Formalin-fixed paraffin-embedded (FFPE) tissue blocks and associated de-identified clinical data were obtained from the Cooperative Human Tissue Network (CHTN), a National Cancer Institute-supported biorepository that prospectively collects specimens from multiple academic medical centers. Samples represented DCIS diagnoses from 2005–2021.From 51 screened subjects, 44 met all criteria and comprised the analytic cohort (**Fig. 1**, **Supplementary Table S1**).

Inclusion criteria: (i) histologically confirmed pure DCIS at index diagnosis; (ii) adequate FFPE tissue for immunohistochemistry (IHC); (iii) clinical follow-up documenting disease status; (iv) complete pathology records including histologic grade.
Exclusion criteria: (i) concurrent invasive carcinoma at index diagnosis; (ii) prior invasive breast cancer; (iii) insufficient tissue quantity/quality for biomarker assessment; (iv) inadequate evaluable DCIS regions for scoring; (v) inadequate follow-up.

Seven subjects were excluded: insufficient tissue quality (n=4), inadequate evaluable DCIS for scoring (n=2), and insufficient follow-up (n=1).

Case-control definitions and outcome assessment

Cases (n=24): patients with pure DCIS at diagnosis who subsequently developed histologically confirmed IDC during follow-up (ipsilateral or contralateral breast; chest wall after mastectomy; or regional lymph nodes). Because PM-TRPV4 was hypothesized to report a patient-level mechanosensing state, invasive events were analyzed irrespective of laterality; laterality was evaluated in sensitivity analyses.

Controls (n=20): patients with pure DCIS who remained IDC-free for ≥5 years of documented surveillance, based on clinical examination, imaging, and absence of histologic invasion on any subsequent biopsies.

The primary endpoint was time from index DCIS diagnosis to the first invasive event as defined above; patients without an event were censored at last disease-free contact.

Clinical data abstraction

All patients in this study were female. Clinical and pathologic variables abstracted from records included age, self-reported race/ethnicity, histologic grade at diagnosis, estrogen receptor (ER) and progesterone receptor (PR) status, surgical treatment (breast-conserving surgery vs mastectomy), receipt of adjuvant radiation, and comorbidities (cardiovascular disease, metabolic disease, smoking history). ER/PR were determined by clinical IHC at diagnosis; hormone receptor data were available for 42/44 patients (2 missing). Median age at diagnosis was 62 years (range, 39–79). Histologic grade was called as low, intermediate, or high by standard criteria and was also collapsed a priori to a binary variable: high grade (HG) vs lower grade (intermediate+low).

Immunohistochemistry for TRPV4 and image acquisition

IHC was performed on 4-µm FFPE sections using a Ventana Discovery Ultra platform (Roche Cat# 760-4311, RRID:AB_2811043). Protocol: deparaffinization (EZ Prep), heat-induced epitope retrieval with Cell Conditioner 1 (CC1; Tris-EDTA pH 8.0, 64 min at 95 °C), endogenous peroxidase block (CM1, 8 min), primary antibody incubation with anti-TRPV4 (Abcam Cat# ab39260, RRID:AB_1143677, anti-rabbit, 1:40, 60 min, room temperature), detection with DISCOVERY OmniMap anti-rabbit HRP (Roche Cat# 760-4311, RRID:AB_2811043) and ChromoMap DAB (Roche Cat# 05266645001), hematoxylin counterstain (8 min) with bluing, dehydration, xylene clearing, and permanent mounting. Each run included positive-control tissue and negative controls (primary omitted). Whole-slide images were scanned on a Hamamatsu NanoZoomer at 20× (0.46 µm/pixel).

PM-TRPV4 scoring rubric and blinding

PM-TRPV4 localization was scored on a five-level ordinal scale incorporating (1) % DCIS epithelial cells with membranous TRPV4 staining, (2) circumferential PM coverage, and (3) staining intensity:

0 (negative): <5% cells; incomplete/absent membrane; faint/absent intensity.

0–1+ (trace): 5–<10% cells; incomplete membrane; faint intensity (below the 1+ threshold).

1+ (low-positive): ≥10% cells; partial–complete membrane; weak to focally moderate intensity.

2+ (moderate-positive): ≥10% cells with ≥50% circumferential coverage; moderate intensity.

3+ (strong-positive): ≥10% cells with ≥50% circumferential coverage; strong intensity.

Three board-certified breast pathologists independently scored 225 image fields from 44 patients, blinded to outcomes, clinical covariates, one another's scores, and grade assignments. For primary analyses, scores were dichotomized a priori:

PM-TRPV4 positive (PM+): if any rater assigned ≥1+, or if all three raters unanimously assigned 0–1+ (trace).

PM-TRPV4 negative (PM–): if all three raters assigned 0, or any mixture of 0 and 0–1+ (discordant trace signal).

This rule prioritizes definite PM relocalization while conservatively classifying ambiguous faint/discordant signal as negative; unanimous trace was treated as biologically positive.

Interobserver agreement: Agreement on the five-level scale was quantified using weighted Fleiss' κ (linear weights) and unweighted Fleiss' κ; pairwise agreement was summarized with weighted

Cohen's κ. 95% CIs were obtained from asymptotic variance; exact agreement proportions (3/3 and 2/3 majority) were tabulated.

Statistical analysis
All tests were two-sided with α=0.05. Analyses used MATLAB R2022a (MathWorks, RRID: SCR_001622) and Python 3.12 (python-bx RRID: SCR_024202, SciPy 1.16.2 RRID: SCR_008058, NumPy: 2.0.2 RRID: SCR_008633). Continuous variables are summarized as median or mean ± SD (or SE); categorical variables as counts (%).

Time-to-event analyses
IDC-free survival was estimated by Kaplan–Meier with 95% CIs by Greenwood and compared using the log-rank test. Cox proportional-hazards models reported hazard ratios (HRs) with 95% Wald CIs and Wald p-values. Ties were handled using the Efron method. Proportional-hazards (PH) assumptions were assessed with Schoenfeld residuals (global and covariate-specific) and inspection of log(–log) curves.

Prespecified models:
Univariable: PM-TRPV4 (primary predictor).
Univariable: histologic grade (high vs lower).
Multivariable: PM-TRPV4 + histologic grade.
Multivariable: PM-TRPV4 + ER status.
Multivariable (fully adjusted): PM-TRPV4 + histologic grade + ER status.

Case-control (2×2) association analyses
To complement survival analyses, Fisher's exact tests (two-sided) were applied to 2×2 tables with odds ratios (ORs) and 95% CIs computed by the Woolf logit method with Haldane–Anscombe correction for zero cells. A prespecified one-sided Fisher test was additionally performed for the directional hypothesis that PM-TRPV4 relocalization increases progression risk. Because case–control sampling fixes the case:control ratio, absolute risk metrics (PPV/NPV/accuracy) are not estimable and were not reported. Treatment-selection and laterality checks used the same approach and are provided in **Supplementary Tables S3–S6.**

Data Availability
De-identified clinical variables are available from the corresponding author upon reasonable request, subject to institutional data-sharing policies and IRB approval. Anonymized scoring results supporting the findings of this study are provided as Supplementary Data. All analysis scripts are publicly available at the ichung-lab GitHub repository (ichung-lab/Longitudinal, /code).

Results
Patient characteristics
From 51 retrospectively identified patients with pure DCIS, 44 were included after exclusions for poor tissue quality (n=4), insufficient evaluable DCIS regions (n=2), or inadequate follow-up (n=1) (**Fig. 1**; **Table 1**). Median age at diagnosis was 62 years (range, 39–79). Race: White 30/44 (68.2%), Black 10/44 (22.7%), Asian 1/44 (2.3%), other/unknown 3/44 (6.8%). Nuclear grade: high 18/44 (40.9%), intermediate 14/44 (31.8%), low 12/44 (27.3%). ER status was available for 42/44 (ER+ 35/42, 83.3%). Primary surgery: lumpectomy 32/44 (72.7%), mastectomy 11/44 (25.0%) (other/unknown 1/44, 2.3%). By design, 24 were progressors and 20 non-progressors with ≥5 years of disease-free surveillance (**Supplementary Table S1**).

PM-TRPV4 scoring and inter-observer agreement

PM-TRPV4 localization was assessed on whole-slide images using a prespecified five-level rubric (0, 0–1+, 1+, 2+, 3+; **Fig. 2A–E**), based on the proportion of DCIS cells exhibiting membranous staining, circumferential PM coverage, and staining intensity. Three board-certified pathologists independently scored 225 image fields from 44 patients, blinded to clinical outcomes. For primary analyses, scores were dichotomized a priori: PM-TRPV4 positive if ≥1 rater assigned ≥1+ or if all three raters unanimously assigned 0–1 (indicating consistent faint membranous signal); PM-TRPV4 negative if all three raters assigned 0 or if scores were any mixture of 0 and 0–1 (discordant faint signal). This dichotomization prioritizes detection of definite PM relocalization while conservatively classifying ambiguous cases as negative (see **Supplementary Data S1** for score-driving ROI images for each case).

Score distributions are shown in **Fig. 2F** (overall) and **Fig. 2G** (stratified by grade). Interobserver agreement on the five-level ordinal scale was almost perfect (linearly weighted Fleiss' κ=0.823, 95% CI 0.777–0.863, p<0.001; unweighted Fleiss' κ=0.728, 95% CI 0.639–0.818) (**Supplementary Fig. S1**; see **Supplementary Data S2** for indexed scores for all 225 ROIs). Observed agreement was 80.7%, with exact 3/3 rater concordance in 71.1% of cases (160/225) and 2/3 majority agreement in 28.9% (65/225). Pairwise weighted Cohen's κ values ranged from 0.731 to 0.996, with near-perfect agreement between two of the three raters (κ=0.996). After dichotomization to PM+/PM–, binary classification showed very high agreement (Fleiss' κ=0.851).

In pro-invasive DCIS cells, crowding-induced mechanical stress in confined ducts drives TRPV4 relocalization to the plasma membrane (27); accordingly, PM-TRPV4 serves as a functional readout of pro-invasive mechanotransduction. **Fig. 2H** reports image-level rates (scored fields), not patient counts: 28.6% (95% CI 16.3–45.1%) in low-grade (n=35), 67.6% (59.5–74.8%) in intermediate-grade (n=139), and 74.5% (61.1–84.5%) in high-grade DCIS (n=51), reflecting image-level counts, demonstrating a significant increasing trend across grades (Cochran–Armitage z=4.03, $p=5.6\times10^{-5}$; Spearman ρ=0.204, p=0.002). We therefore examined PM-TRPV4's association with IDC progression.

PM-TRPV4 independently predicts IDC-free survival

In the cohort of 44 patients (24 progression events; median follow-up 7.6 years, range 0.4–14.9 years), Kaplan–Meier curves showed visible separation by PM-TRPV4 status (**Fig. 3A**, **Table 2**). PM-TRPV4–positive tumors had inferior IDC-free survival compared with PM-TRPV4–negative tumors (log-rank p=0.0396). By contrast, histologic grade was not associated with outcome in this dataset (**Fig. 3B**, **Table 2**), with overlapping curves for high vs lower grade disease (log-rank p=0.7199).

Follow-up time (mean ± SE) was shorter in PM-TRPV4+ than PM-TRPV4− cases (7.2 ± 0.6 vs 9.6 ± 1.3 years), but the difference was not significant (two-sample t-test p=0.077; **Fig. 3C**), arguing against differential observation time as a driver of the survival difference.

Effect sizes from Cox models are summarized in the forest plots. In univariable Cox (**Fig. 3D**), PM-TRPV4+ was associated with higher hazard of progression (HR=3.09; 95% CI 0.84–11.40; Wald p=0.0908), whereas histologic grade was not significant (high vs lower: HR=0.79; 95% CI 0.34–1.80; Wald p=0.5677). In a multivariable Cox model including PM-TRPV4, histologic grade, and ER status (**Fig. 3E**, **Table 2**), PM-TRPV4 remained independently associated with shorter IDC-free survival (adjusted HR=3.77; 95% CI 1.01–14.12; Wald p=0.0489). Neither high grade (adjusted HR=0.79; 95% CI 0.34–1.80; Wald p=0.5677) nor ER positivity (adjusted HR=1.99; 95% CI 0.71–5.59; Wald p=0.1893) was significant after adjustment.

Testing of proportional hazards assumptions using Schoenfeld residuals indicated that the assumption was satisfied for PM-TRPV4 (p=0.67) and histologic grade (p=0.39). Although evidence of non-proportionality was detected for ER status (p=0.0001), ER was not prognostic (p=0.19 as noted above), and this violation does not affect interpretation of the primary PM-TRPV4 findings.

Exploratory grade-stratified analyses (**Fig. S2**; **Supplementary Table S2**) suggested a larger PM-TRPV4 effect within lower-grade DCIS, whereas the high-grade subgroup was imprecise due to very small PM-TRPV4− numbers. In lower-grade DCIS, PM-TRPV4+ cases had higher progression risk (**Fig. S2A,C**; log-rank p=0.0703; HR=3.24; 95% CI 0.85–12.41; Wald p=0.0859) and higher raw progression rate (14/18 [77.8%] vs 2/8 [25.0%], **Fig. S2D**). The high-grade subgroup was underpowered (only one PM-TRPV4− case) and did not show a significant difference (**Fig. S2B,C**; log-rank p=0.2280; HR=1.85; 95% CI 0.11–32.06; Wald p=0.6723). Overall, PM-TRPV4 positivity is an independent predictor of poorer IDC-free survival in this cohort.

Univariable analysis (**Supplementary Table S3**) showed that plasma-membrane TRPV4 (PM-TRPV4) positivity was associated with higher odds of invasive progression (OR = 5.92; 95% CI 1.07–32.90; p = 0.057, two-sided Fisher's exact test). In contrast, histologic grade (OR = 0.50; p = 0.36), ER status (OR = 1.78; p = 0.68), and comorbid factors, including cardiovascular disease, metabolic disorder, or smoking history, were not associated with progression. These findings are directionally concordant with the survival analyses and support PM-TRPV4 as a prognostic biomarker.

Treatment and site sensitivity analyses

To evaluate potential treatment-selection bias, we compared PM-TRPV4 status with surgical management (intensive treatment defined as lumpectomy + radiation or mastectomy). PM-TRPV4 was not associated with receipt of intensive therapy versus lumpectomy alone (OR = 2.33; 95% CI 0.45–12.06; two-sided Fisher's p = 0.367; **Supplementary Table S4**). Surgical intensity also was not associated with progression (OR = 0.50; 95% CI 0.11–2.33; two-sided Fisher's p = 0.467; **Supplementary Table S5**). Among progressed cases, ipsilateral and contralateral events occurred with similar frequency (13 vs 10; **Supplementary Table S6**) and showed no association with PM-TRPV4 status (OR = 0.20; 95% CI 0.00–0.87; two-sided Fisher's p = 0.482; **Supplementary Table S7**). Together, these analyses indicate that the PM-TRPV4 survival signal is not explained by treatment choice or event laterality.

DISCUSSION

In this single-institution case–control series of 44 patients with pure DCIS (24 progressors; median follow-up 7.6 years), plasma-membrane relocalization of TRPV4 (PM-TRPV4) was associated with inferior IDC-free survival and remained independently prognostic after accounting for histologic grade and ER status. Kaplan–Meier curves separated by PM-TRPV4 status (log-rank p=0.0396), and in multivariable Cox regression PM-TRPV4 positivity was linked to shorter time to invasion (adjusted HR=3.77; 95% CI 1.01–14.12; Wald p=0.0489). By contrast, histologic grade was not prognostic in this cohort (adjusted HR=0.79; 95% CI 0.34–1.80; p=0.5677), underscoring a disconnect between nuclear morphology and the biology that drives invasion. Odds-based analyses pointed in the same direction: PM-TRPV4 positivity was associated with higher odds of progression (OR=5.92; 95% CI 1.07–32.90; two-sided Fisher p=0.057), consistent with the survival signal. Notably, the strongest discrimination appeared in lower-grade disease (**Fig. S2; Supplementary Table S2**): among intermediate+low grade cases, effect sizes were large (e.g., OR=10.50; 95% CI 1.54–71.76; p=0.016; HR=3.24; 95% CI 0.85–12.41; p=0.0859), whereas the high-grade stratum was underpowered due to very few PM-negative cases.

Our mechanistic data provide a coherent basis for the clinical findings. Crowding within confined ducts perturbs mechanotransduction, inactivates PM-resident TRPV4, lowers intracellular Ca^{2+}, and triggers compensatory trafficking of intracellular inactive TRPV4 back to the PM (27). This stress-induced relocalization marks engagement of a pro-invasive mechanosensing program that morphology or bulk protein levels cannot capture. Accordingly, a simple IHC readout of where TRPV4 resides, PM vs cytoplasm, serves as a functional biomarker of pathway state rather than a surrogate for tumor grade. Consistent with a patient-level biology, treatment- and site-sensitivity analyses showed no association between PM-TRPV4 and receipt of more intensive therapy, no link between surgical intensity and progression, and no relationship between event laterality (ipsilateral vs contralateral) and PM-TRPV4 status (**Supplementary Tables S3–S6**). Exploratory sensitivity analyses showed no significant associations between PM-TRPV4 and treatment selection (OR=2.33, p=0.37) or event laterality among progressors (OR=0.20, p=0.48), though wide confidence intervals preclude definitive conclusions about potential confounding (**Supplementary Tables S4–S7**).

Crucially, the assay appears feasible and reproducible. Using a prespecified five-level membrane-localization rubric specific to TRPV4, incorporating percentage of positive cells, circumferential membrane coverage, and staining intensity, three breast pathologists achieved almost-perfect agreement on the ordinal scale (weighted Fleiss' κ=0.823; 95% CI 0.777–0.863), with even higher agreement after dichotomization to PM+/PM– (Fleiss' κ=0.851). This reliability, together with routine FFPE sections and standard IHC platforms, supports portability beyond specialized centers and a realistic path to multi-site implementation with appropriate anchors and training.

This study has limitations. It is a single-institution, retrospective case–control series with a modest sample (N=44; 24 events), yielding wide CIs and limiting subgroup precision, particularly where PM-TRPV4 negative high-grade cases were rare. Controls required ≥5 years disease-free follow-up, yet invasive events can accrue beyond 10 years (31-37); nonetheless, PM-TRPV4 negative patients had longer disease-free surveillance than PM-positive patients, arguing against differential observation as the driver of the survival separation. Case–control sampling fixes the case:control ratio and precludes estimation of absolute risks or calibration (e.g., PPV/NPV); we therefore focused on time-to-event measures and ORs, which remain valid under this design. Although treatment-selection and laterality sensitivity analyses were negative, residual confounding and selection bias cannot be excluded. Assay generalizability requires inter-laboratory threshold calibration because staining/scoring were optimized on a single platform with one antibody and local anchors. Receptor data were missing for two patients, and no external validation cohort was available. Despite these constraints, analyses were prespecified and parsimonious, interobserver agreement was high, and findings were directionally consistent across sensitivity analyses, lending robustness to the main conclusion.

Clinically, these data nominate PM-TRPV4 as a mechanism-informed biomarker that can complement grading, particularly in lower-grade DCIS where morphology alone underserves risk stratification. If validated, PM-TRPV4 could help identify biologically active lesions for closer monitoring or intervention, while supporting de-escalation in PM-negative lower-grade disease. The pragmatic next steps are clear: multi-institutional, prospectively followed cohorts with standardized staining/scoring and ≥10-year surveillance; head-to-head testing alongside established tools (e.g., DCISionRT (16,38), clinicopathologic nomograms (39,40)) to quantify incremental value; and integration as an exploratory endpoint in active-surveillance/de-escalation trials. Taken together, our findings provide clinical proof-of-concept that a simple, robust IHC readout of TRPV4 localization captures pro-invasive mechanotransduction and offers independent prognostic information beyond grade and ER in DCIS.

In summary, plasma-membrane TRPV4 localization provides independent prognostic information in DCIS beyond conventional histologic grade and ER status, with particular utility in lower-grade disease where risk stratification is most challenging. The biomarker's mechanistic foundation, combined with high interobserver reliability (κ=0.823) and compatibility with routine pathology workflows, supports its potential for clinical translation. While these hypothesis-generating findings require multi-institutional validation with standardized protocols and extended follow-up, they establish proof-of-concept that a simple functional readout of mechanotransduction pathway engagement can augment morphology-based risk assessment and inform personalized DCIS management.

Acknowledgments

This work was supported by the Elsa Pardee Foundation Award, the George Washington University Technology Maturation Award, the George Washington Cross-Disciplinary Research Fund, the George Washington Cancer Center, and the Katzen Cancer Research Pilot Award. Tissue samples were provided by the Cooperative Human Tissue Network (CHTN), which is funded by the National Cancer Institute; other investigators may have received specimens from the same subjects. We thank Rebecca Blackwell for case identification; Dr. Christopher Moskaluk (CHTN, University of Virginia) for histologic review; and Dr. Patcharin Pramoonjago and Barushi Amarasinghe (Biorepository and Tissue Research Facility, University of Virginia) for tissue staining.

Author Contributions

C. Chan: Data curation, visualization (IHC figure assembly); E. Arbzadeh: Methodology (scoring rubric), investigation (ROI annotation; TRPV4 scoring), validation; S. Samankan: Methodology (scoring rubric), investigation (ROI annotation; TRPV4 scoring), validation; P. Latham: Methodology (scoring rubric), investigation (TRPV4 scoring), validation; A. Schwartz: Methodology (scoring rubric), resources/pathology oversight, writing–review and editing. R. Du: Formal analysis (descriptive statistics); I. Chung: Conceptualization, study design, methodology, formal analysis, supervision, project administration, funding acquisition, writing–original draft, writing–review and editing.

Competing Interests

I. Chung is an inventor on U.S. Patent No. 12,013,398 related to plasma-membrane localization–based diagnostics; the patent is assigned to The George Washington University. The patent has not been licensed, and no commercial products are currently in development. No authors have received or will receive financial compensation related to this patent. No industry funding supported this work.

References

1. Allred DC. Ductal carcinoma in situ: terminology, classification, and natural history. *J Natl Cancer Inst Monogr* 2010;**2010**(41):134-8 doi 10.1093/jncimonographs/lgq035.
2. Bocker W. Preneoplasia of the breast. *Verh Dtsch Ges Pathol* 1997;**81**:502-13.
3. Gudjonsson T, Adriance MC, Sternlicht MD, Petersen OW, Bissell MJ. Myoepithelial cells: Their origin and function in breast morphogenesis and neoplasia. *J Mammary Gland Biol* 2005;**10**(3):261-72 doi 10.1007/s10911-005-9586-4.
4. Siegel RL, Kratzer TB, Giaquinto AN, Sung H, Jemal A. Cancer statistics, 2025. *CA Cancer J Clin* 2025;**75**(1):10-45 doi 10.3322/caac.21871.

5. van Seijen M, Lips EH, Thompson AM, Nik-Zainal S, Futreal A, Hwang ES*, et al.* Ductal carcinoma in situ: to treat or not to treat, that is the question. *Br J Cancer* 2019;**121**(4):285-92 doi 10.1038/s41416-019-0478-6.
6. Kumar AS, Bhatia V, Henderson IC. Overdiagnosis and overtreatment of breast cancer: rates of ductal carcinoma in situ: a US perspective. *Breast Cancer Res* 2005;**7**(6):271-5 doi 10.1186/bcr1346.
7. Baxter NN, Virnig BA, Durham SB, Tuttle TM. Trends in the treatment of ductal carcinoma in situ of the breast. *J Natl Cancer Inst* 2004;**96**(6):443-8 doi 10.1093/jnci/djh069.
8. Srivastava S, Koay EJ, Borowsky AD, De Marzo AM, Ghosh S, Wagner PD*, et al.* Cancer overdiagnosis: a biological challenge and clinical dilemma. *Nat Rev Cancer* 2019;**19**(6):349-58 doi 10.1038/s41568-019-0142-8.
9. Ryser MD, Horton JK, Hwang ES. How Low Can We Go-and Should We? Risk Reduction for Minimal-Volume DCIS. *Ann Surg Oncol* 2018;**25**(2):354-5 doi 10.1245/s10434-017-6128-4.
10. Ryser MD, Weaver DL, Zhao F, Worni M, Grimm LJ, Gulati R*, et al.* Cancer Outcomes in DCIS Patients Without Locoregional Treatment. *J Natl Cancer Inst* 2019;**111**(9):952-60 doi 10.1093/jnci/djy220.
11. Hanna WM, Parra-Herran C, Lu FI, Slodkowska E, Rakovitch E, Nofech-Mozes S. Ductal carcinoma in situ of the breast: an update for the pathologist in the era of individualized risk assessment and tailored therapies. *Mod Pathol* 2019;**32**(7):896-915 doi 10.1038/s41379-019-0204-1.
12. Worni M, Akushevich I, Greenup R, Sarma D, Ryser MD, Myers ER*, et al.* Trends in Treatment Patterns and Outcomes for Ductal Carcinoma In Situ. *J Natl Cancer Inst* 2015;**107**(12):djv263 doi 10.1093/jnci/djv263.
13. Maxwell AJ, Clements K, Hilton B, Dodwell DJ, Evans A, Kearins O*, et al.* Risk factors for the development of invasive cancer in unresected ductal carcinoma in situ. *Eur J Surg Oncol* 2018;**44**(4):429-35 doi 10.1016/j.ejso.2017.12.007.
14. Collins LC, Tamimi RM, Baer HJ, Connolly JL, Colditz GA, Schnitt SJ. Outcome of patients with ductal carcinoma in situ untreated after diagnostic biopsy: results from the Nurses' Health Study. *Cancer* 2005;**103**(9):1778-84 doi 10.1002/cncr.20979.
15. Kerlikowske K, Molinaro A, Cha I, Ljung BM, Ernster VL, Stewart K*, et al.* Characteristics associated with recurrence among women with ductal carcinoma in situ treated by lumpectomy. *J Natl Cancer Inst* 2003;**95**(22):1692-702 doi 10.1093/jnci/djg097.
16. Rakovitch E, Nofech-Mozes S, Hanna W, Baehner FL, Saskin R, Butler SM*, et al.* A population-based validation study of the DCIS Score predicting recurrence risk in individuals treated by breast-conserving surgery alone. *Breast Cancer Res Treat* 2015;**152**(2):389-98 doi 10.1007/s10549-015-3464-6.
17. Erbas B, Provenzano E, Armes J, Gertig D. The natural history of ductal carcinoma in situ of the breast: a review. *Breast Cancer Res Treat* 2006;**97**(2):135-44 doi 10.1007/s10549-005-9101-z.
18. Sanders ME, Schuyler PA, Dupont WD, Page DL. The natural history of low-grade ductal carcinoma in situ of the breast in women treated by biopsy only revealed over 30 years of long-term follow-up. *Cancer* 2005;**103**(12):2481-4 doi 10.1002/cncr.21069.
19. Hulahan TS, Spruill L, Wallace EN, Park Y, West RB, Marks JR*, et al.* Extracellular Microenvironment Alterations in Ductal Carcinoma In Situ and Invasive Breast Cancer Pathologies by Multiplexed Spatial Proteomics. *Int J Mol Sci* 2024;**25**(12) doi 10.3390/ijms25126748.
20. Ma A, Xiang L, Yuan J, Wang Q, Zhao L, Yan H. Spatial Transcriptomics Decodes Breast Cancer Microenvironment Heterogeneity: From Multidimensional Dynamic Profiling to Precision Therapy Blueprint Construction. *Biomolecules* 2025;**15**(8) doi 10.3390/biom15081067.

21. Strand SH, Houlahan KE, Branch V, King LM, Lynch T, Rivero-Guitiérrez B*, et al.* Analysis of ductal carcinoma in situ by self-reported race reveals molecular differences related to outcome. *Breast Cancer Res* 2024;**26**(1):127 doi 10.1186/s13058-024-01885-8.
22. Hwang ES, Hyslop T, Lynch T, Frank E, Pinto D, Basila D*, et al.* The COMET (Comparison of Operative versus Monitoring and Endocrine Therapy) trial: a phase III randomised controlled clinical trial for low-risk ductal carcinoma in situ (DCIS). *BMJ Open* 2019;**9**(3):e026797 doi 10.1136/bmjopen-2018-026797.
23. Elshof LE, Tryfonidis K, Slaets L, van Leeuwen-Stok AE, Skinner VP, Dif N*, et al.* Feasibility of a prospective, randomised, open-label, international multicentre, phase III, non-inferiority trial to assess the safety of active surveillance for low risk ductal carcinoma in situ - The LORD study. *Eur J Cancer* 2015;**51**(12):1497-510 doi 10.1016/j.ejca.2015.05.008.
24. Francis A, Thomas J, Fallowfield L, Wallis M, Bartlett JM, Brookes C*, et al.* Addressing overtreatment of screen detected DCIS; the LORIS trial. *Eur J Cancer* 2015;**51**(16):2296-303 doi 10.1016/j.ejca.2015.07.017.
25. Partridge AH, Hyslop T, Rosenberg SM, Bennett AV, Drier S, Jonsson M*, et al.* Patient-Reported Outcomes for Low-Risk Ductal Carcinoma In Situ: A Secondary Analysis of the COMET Randomized Clinical Trial. *JAMA Oncol* 2025;**11**(3):300-9 doi 10.1001/jamaoncol.2024.6556.
26. Shah C, Bremer T, Cox C, Whitworth P, Patel R, Patel A*, et al.* The Clinical Utility of DCISionRT(®) on Radiation Therapy Decision Making in Patients with Ductal Carcinoma In Situ Following Breast-Conserving Surgery. *Ann Surg Oncol* 2021;**28**(11):5974-84 doi 10.1245/s10434-021-09903-1.
27. Bu X, Ashby N, Vitali T, Lee S, Gottumukkala A, Yun K*, et al.* Cell crowding activates pro-invasive mechanotransduction pathway in high-grade DCIS via TRPV4 inhibition and cell volume reduction. *eLife* 2025:13:RP100490 doi 10.7554/eLife.100490.4.
28. Rosenbaum T, Benitez-Angeles M, Sanchez-Hernandez R, Morales-Lazaro SL, Hiriart M, Morales-Buenrostro LE*, et al.* TRPV4: A Physio and Pathophysiologically Significant Ion Channel. *Int J Mol Sci* 2020;**21**(11) doi 10.3390/ijms21113837.
29. White JP, Cibelli M, Urban L, Nilius B, McGeown JG, Nagy I. TRPV4: Molecular Conductor of a Diverse Orchestra. *Physiol Rev* 2016;**96**(3):911-73 doi 10.1152/physrev.00016.2015.
30. Hua R, Jiang JX. How cell crowding causes cancer cells to spread. *eLife* 2025;**14**:e106768 doi 10.7554/eLife.106768.
31. Solin LJ, Kurtz J, Fourquet A, Amalric R, Recht A, Bornstein BA*, et al.* Fifteen-year results of breast-conserving surgery and definitive breast irradiation for the treatment of ductal carcinoma in situ of the breast. *J Clin Oncol* 1996;**14**(3):754-63 doi 10.1200/jco.1996.14.3.754.
32. Wallis MG, Clements K, Kearins O, Ball G, Macartney J, Lawrence GM. The effect of DCIS grade on rate, type and time to recurrence after 15 years of follow-up of screen-detected DCIS. *Br J Cancer* 2012;**106**(10):1611-7 doi 10.1038/bjc.2012.151.
33. Weinmann S, Leo MC, Francisco M, Jenkins CL, Barry T, Leesman G*, et al.* Validation of a Ductal Carcinoma In Situ Biomarker Profile for Risk of Recurrence after Breast-Conserving Surgery with and without Radiotherapy. *Clin Cancer Res* 2020;**26**(15):4054-63 doi 10.1158/1078-0432.Ccr-19-1152.
34. Donker M, Litière S, Werutsky G, Julien JP, Fentiman IS, Agresti R*, et al.* Breast-conserving treatment with or without radiotherapy in ductal carcinoma In Situ: 15-year recurrence rates and outcome after a recurrence, from the EORTC 10853 randomized phase III trial. *J Clin Oncol* 2013;**31**(32):4054-9 doi 10.1200/jco.2013.49.5077.
35. Wärnberg F, Garmo H, Emdin S, Hedberg V, Adwall L, Sandelin K*, et al.* Effect of radiotherapy after breast-conserving surgery for ductal carcinoma in situ: 20 years follow-

up in the randomized SweDCIS Trial. *J Clin Oncol* 2014;**32**(32):3613-8 doi 10.1200/jco.2014.56.2595.

36. Wapnir IL, Dignam JJ, Fisher B, Mamounas EP, Anderson SJ, Julian TB*, et al.* Long-term outcomes of invasive ipsilateral breast tumor recurrences after lumpectomy in NSABP B-17 and B-24 randomized clinical trials for DCIS. *J Natl Cancer Inst* 2011;**103**(6):478-88 doi 10.1093/jnci/djr027.
37. Barrio AV, Van Zee KJ. Controversies in the Treatment of Ductal Carcinoma in Situ. *Annu Rev Med* 2017;**68**:197-211 doi 10.1146/annurev-med-050715-104920.
38. Bremer T, Whitworth PW, Patel R, Savala J, Barry T, Lyle S*, et al.* A Biological Signature for Breast Ductal Carcinoma In Situ to Predict Radiotherapy Benefit and Assess Recurrence Risk. *Clin Cancer Res* 2018;**24**(23):5895-901 doi 10.1158/1078-0432.Ccr-18-0842.
39. Rudloff U, Jacks LM, Goldberg JI, Wynveen CA, Brogi E, Patil S*, et al.* Nomogram for predicting the risk of local recurrence after breast-conserving surgery for ductal carcinoma in situ. *J Clin Oncol* 2010;**28**(23):3762-9 doi 10.1200/jco.2009.26.8847.
40. Silverstein MJ, Lagios MD, Groshen S, Waisman JR, Lewinsky BS, Martino S*, et al.* The influence of margin width on local control of ductal carcinoma in situ of the breast. *N Engl J Med* 1999;**340**(19):1455-61 doi 10.1056/nejm199905133401902.

`

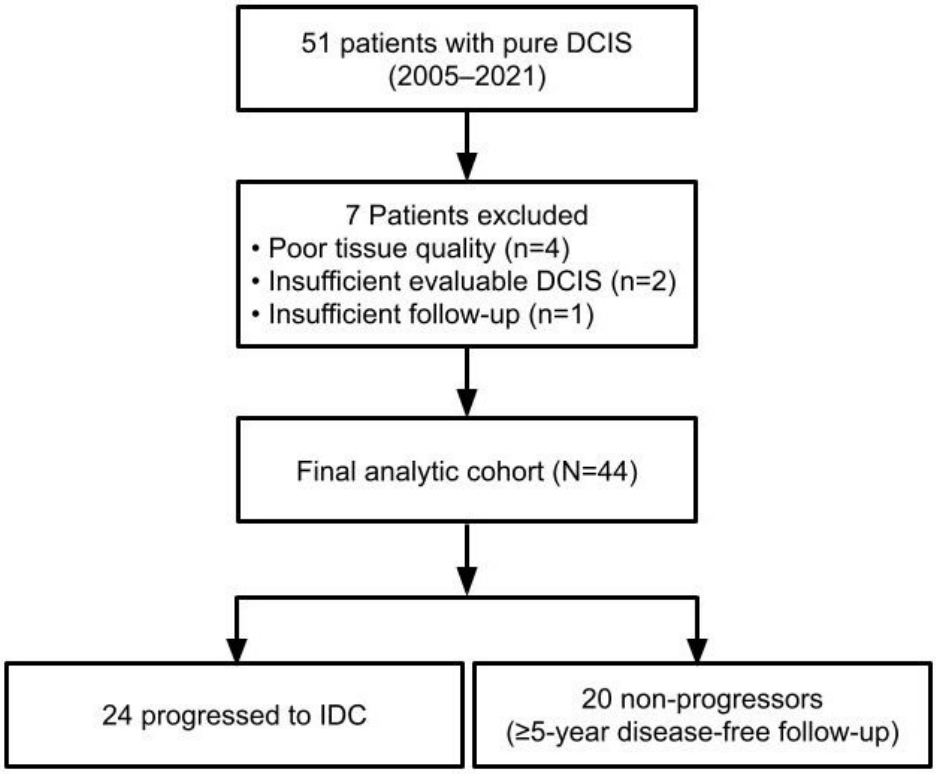

Figure 1. Patient selection and study flow diagram.

Flow diagram showing patient selection for DCIS progression analysis. From an initial cohort of 51 retrospective FFPE slides with pure ductal carcinoma in situ, 7 cases were excluded due to inadequate tissue quality (n=4), insufficient evaluable DCIS regions (n=2), or short follow-up (n=1), yielding a final analytical cohort of 44 patients. Twenty-four patients (54.5%) experienced progression to invasive carcinoma during follow-up, while 20 patients (45.5%) remained progression-free with minimum 5-year disease-free surveillance.

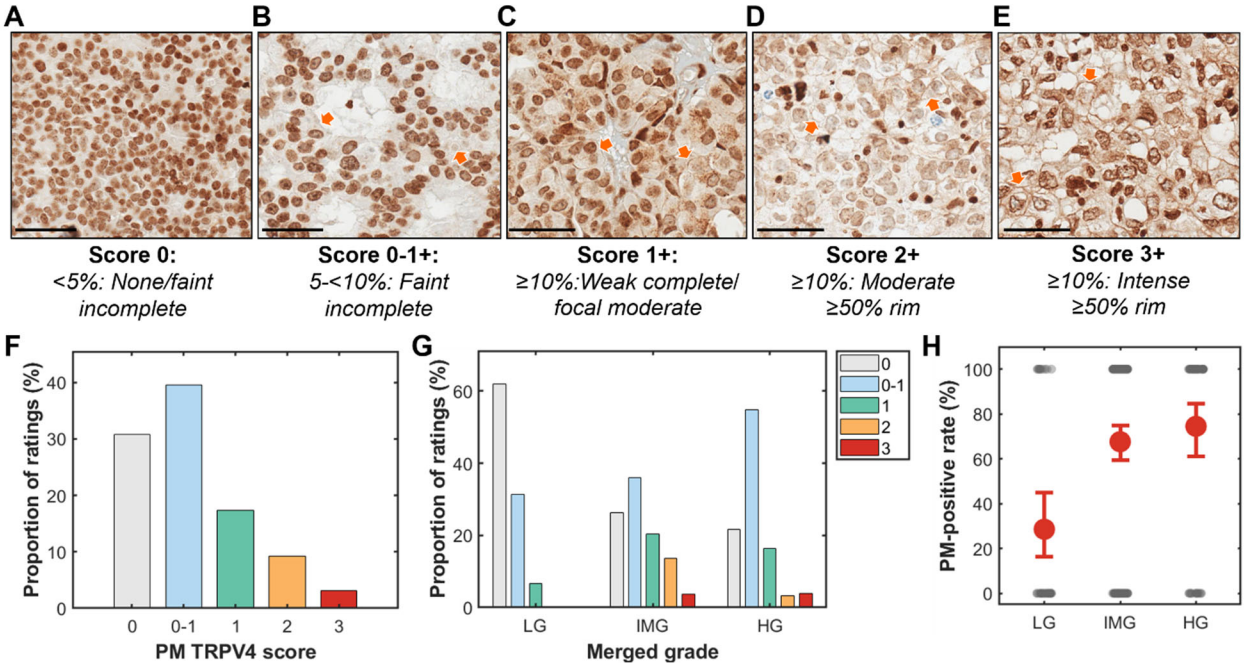

Figure 2. PM-TRPV4 Scoring Rubric, Score Distributions, and Association with Grade

(A–E) Representative whole-slide images illustrating the 5-level PM-TRPV4 scoring rubric applied to DCIS epithelial cells. Orange arrows indicate cells with plasma membrane TRPV4 localization.
(A) Score 0: No staining or incomplete and faint PM staining in <5% (rare) DCIS cells**.**
(B) Score 0–1+: Incomplete and faint PM staining in ≥5% and <10% of DCIS cells.
(C) Score 1+: Weak complete to focally moderate PM staining in ≥10% of DCIS cells. PM coverage ranges from partial to complete.
(D) Score 2+: Moderate PM staining with ≥50% circumferential PM coverage in ≥10% of DCIS cells.
(E) Score 3+: Intense PM staining with ≥50% circumferential PM coverage in ≥10% of DCIS cells. Red arrowheads highlight incomplete **(B–C)** versus complete **(D–E)** membrane rims. Scale bars, 100 µm; identical acquisition/display settings.
(F) Overall PM-TRPV4 score distribution across all 225 scored DCIS images from three independent pathologists (675 total ratings). Bars show the proportion of ratings in each score category.
(G) PM-TRPV4 score distributions stratified by histologic grade (LG, low grade; IMG, intermediate grade; HG, high grade). Bars show proportion of ratings in each score category within each grade stratum. Higher scores (2+ and 3+) predominate in intermediate- and high-grade DCIS.
(H) PM-TRPV4 positivity by histologic grade at the image level (fields: low-grade n=35, intermediate n=139, high-grade n=51). These counts reflect scored DCIS image fields, not the number of patients. Error bars = 95% CIs for proportions. Trend tests: Cochran–Armitage z=4.03, $p=5.6\times10^{-5}$; Spearman ρ=0.204, p=0.002.

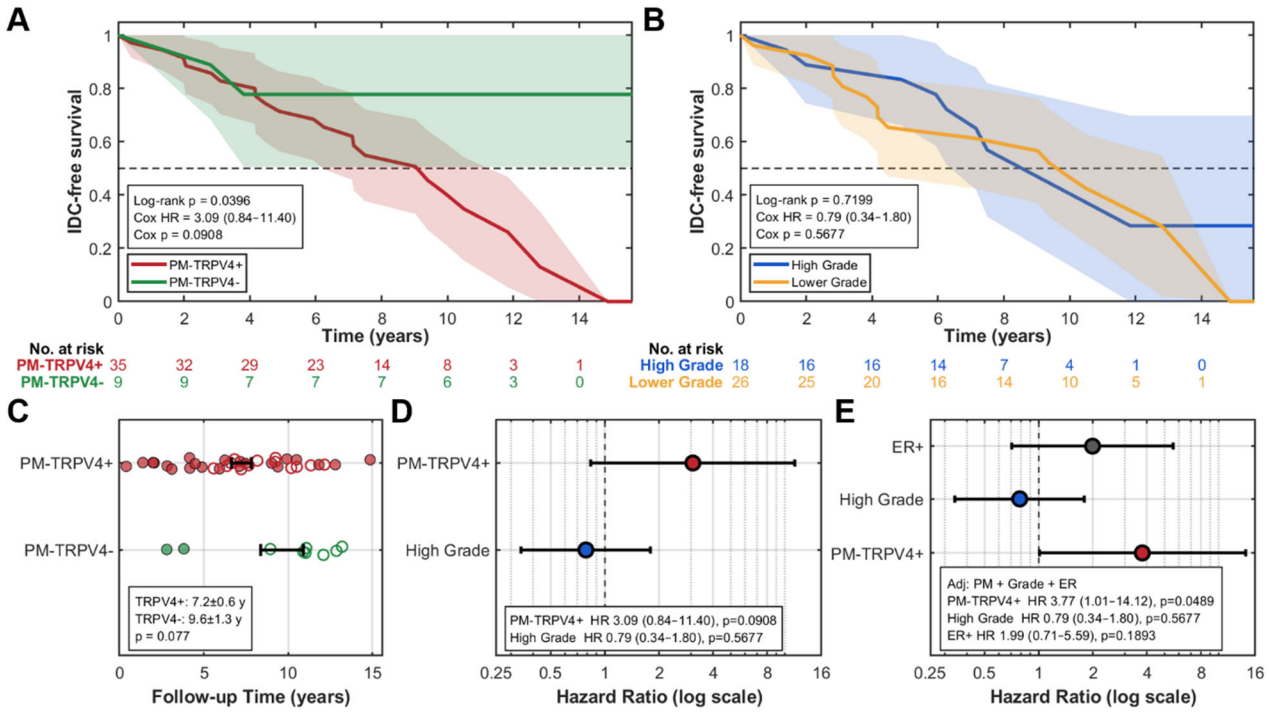

Figure 3. IDC-free survival by PM-TRPV4 status and histologic grade
Cohort: 44 patients; 24 progression events (54.5%); median follow-up 7.6 y (range 0.4–14.9).
(A) Kaplan–Meier curves for IDC-free survival stratified by PM-TRPV4 status in 44 patients (24 events; median follow-up 7.6 y, range 0.4–14.9). PM-TRPV4-positive (red; n=35) had worse survival than PM-TRPV4-negative (green; n=9). Shaded bands are 95% CIs (Greenwood). Dashed line marks 50% survival. Numbers at risk (every 2 y): PM-TRPV4+ 35, 32, 29, 23, 14, 8, 3, 1; PM-TRPV4− 9, 9, 7, 7, 7, 6, 3, 0. Log-rank p=0.0396. Univariable Cox HR=3.09 (95% CI 0.84–11.40), Cox p=0.0908.
(B) Kaplan–Meier curves by histologic grade (blue=High, n=18; orange=Lower, n=26) with the same conventions. Numbers at risk (every 2 y): High 18, 16, 16, 14, 7, 4, 1, 0; Lower 26, 25, 20, 16, 14, 10, 5, 1. Log-rank p=0.7199. Univariable Cox HR=0.79 (95% CI 0.34–1.80), Cox p=0.5677 (High vs Lower).
(C) Follow-up duration by PM-TRPV4 status. Points show individual patients (filled=event; open=censored). Mean ± SE follow-up: PM-TRPV4+ 7.2 ± 0.6 y; PM-TRPV4− 9.6 ± 1.3 y; two-sample t-test p=0.077.
(D) Univariable Cox forest plot on a log scale (vertical dashed line at reference HR=1). PM-TRPV4+: HR=3.09 (95% CI 0.84–11.40), Cox p=0.0908. High Grade: HR=0.79 (95% CI 0.34–1.80), Cox p=0.5677.
(E) Multivariable Cox forest plot adjusted for PM-TRPV4, grade, and ER status (log scale; reference HR=1). ER+: adjusted HR=1.99 (95% CI 0.71–5.59), Cox p=0.1893. High Grade: adjusted HR=0.79 (95% CI 0.34–1.80), Cox p=0.5677. PM-TRPV4+: adjusted HR=3.77 (95% CI 1.01–14.12), Cox p=0.0489. PM-TRPV4 positivity independently predicts worse IDC-free survival (adjusted HR=3.77, p=0.0489) after adjusting for grade and ER status in 44 patients with 24 progression events. Treatment and site sensitivity analyses are provided in **Supplementary Tables S3–S6**; case-level data are provided in **S1.**

Characteristic	**Total (N = 44)**
Ages (39-79 years)	
Age, median	62
Race	
White	30 (68.2%)
Black	10 (22.7%)
Asian	1 (2.3%)
Other	3 (6.8%)
DCIS Grade	
High	18 (40.9%)
Intermediate	14 (31.8%)
Low	12 (27.3%)
ER Status* (n=42)	
Positive	35 (83.3%)
Negative	7 (16.7%)
Treatment	
Lumpectomy	32 (72.7%)
Mastectomy	11 (25.0%)
Radiation	23 (52.3%)
n = 42, after excluding cases with unknown ER status*	

Table 1. Patient demographics and clinical characteristics

Baseline characteristics of patients with pure DCIS (N=44). Data presented as n (%) for categorical variables and median (range) for continuous variables. DCIS grade was determined by board-certified pathologists using standard criteria including nuclear morphology and architectural patterns. Treatment decisions were made according to institutional guidelines and patient preference. *ER status was available for 42 patients.

Variable (reference)	Univariable HR (95% CI)	Univ. p	Adjusted HR (95% CI)	Adj. p
PM-TRPV4+ (vs −)	3.09 (0.84–11.40)	0.0908	**3.77 (1.01–14.12)**	**0.0489**
High grade (vs lower)	0.79 (0.34–1.80)	0.5677	0.79 (0.34–1.80)	0.5677
ER+ (vs ER−)	—	—	1.99 (0.71–5.59)	0.1893

Table 2. Cox models for IDC-free survival (N=44; 24 events)

IDC-free survival was analyzed with Cox proportional-hazards regression. For each predictor, we report (i) univariable estimates and their two-sided Wald p-values (Univ p), and (ii) multivariable estimates (Adjusted HR) from a model including PM-TRPV4 status, histologic grade, and ER status; the associated two-sided Wald p-values are shown as Adj p. Hazard ratios and 95% confidence intervals were computed as $\exp(\beta)$ and $\exp(\beta \pm 1.96\times SE)$. Time-to-event was measured from diagnosis to invasive progression or censoring at last follow-up. Ties were handled using the Efron method. All tests were two-sided with $\alpha=0.05$. (ER was included as a covariate for adjustment and was not prespecified for separate univariable testing.)